Journal of Materials Chemistry A

ROYAL SOCIETY OF CHEMISTRY

PAPER

View Article Online
View Journal | View Issue

Cite this: J. Mater. Chem. A, 2024, 12, 5918

Highly stable poly-nitro components achieved through supramolecular encapsulation†

Jichuan Zhang,[ab] Jinhao Zhang,[b] Jatinder Singh,[a] Wanbao Wu,[c] Richard J. Staples,[d] Jiaheng Zhang *[b] and Jean'ne M. Shreeve *[a]

Received 11th December 2023
Accepted 5th February 2024

DOI: 10.1039/d3ta07665b

rsc.li/materials-a

As representatives of poly-nitro oxidant components, dinitramide [$^{-}N(NO_2)_2$, DN] and nitroformate [$^{-}C(NO_2)_3$, NF] exhibit a very large potential as energetic materials given their highly available oxygen content. However, their low thermal stabilities have always been the main reason limiting their applications. Now, a strategy of encapsulating poly-nitro components through supramolecular self-assembly has been developed; six supramolecular encapsulated structures (two series): MA@DN, MA@NF, MA@TNP; TATOT@DN, TATOT@NF, and TATOT@TNP (Ma: melamine; TATOT: 3,6,7-triamino-7H-[1,2,4]triazolo[5,1-c][1,2,4]-triazole; TNP: 3,4,5-trinitro-pyrazolate) were assembled simply in aqueous solution. Benefiting from the supramolecular structure, and the fixed hydrogen bonds formed between the poly-nitro components and the supramolecular framework, the thermal stability of these poly-nitro components was improved remarkably. Particularly, the decomposition temperatures of MA@DN, MA@NF, and MA@TNP are 243, 225, and 268 °C, respectively, which are the highest decomposition temperatures among these derivatives. Additionally, supramolecules based on TATOT exhibit excellent detonation properties and lower sensitivities to mechanical stimuli, which makes them promising as high energy materials with lower sensitivities. This work provides a new strategy for stabilizing liable components, and as a result, more and more highly energetic and stable materials based on poly-nitro components will be prepared.

Introduction

As representatives of unstable poly-nitro oxidants, dinitramide [$^{-}N(NO_2)_2$, DN][1] and nitroformate [$^{-}C(NO_2)_3$, NF],[2] attract considerable attention as explosives and propellants given their high oxygen content and simple preparation. Over the years, various strategies, including forming salts with nitrogen-rich cations,[3–8] encapsulated by Metal–Organic Frameworks (MOFs),[9] Hydrogen-bonded Organic Frameworks (HOFs),[10] Polymers,[11] *etc.*, have been employed to improve their thermostabilities, the decomposition temperatures of most of the resultant structures are still low (the decomposition temperatures of DN-based derivatives lie between 130–180 °C,[12] and the thermostabilities of NF-based compounds fall between 80–150 °C).[2–9] Nevertheless, it is worth noting that the more hydrogen bonds (HB) fixed on the poly-nitro oxidant with the surrounding molecule/ion, the higher the stability of their derivatives, such as in the salt of TABT-DN (TABT: 4,4′,5,5′-tetraamino-3,3′-bi-1,2,4-triazolate).[13] All of the oxygen atoms of DN were fixed by hydrogen bonds (HBs), leading to a decomposition temperature of 201 °C; in the structure of MA-NF, 5 of these atoms of NF were fixed by 10 HBs, which give raise to a thermal stability of 143 °C.[3] Recently, our studies have shown that except for the HBs generated between the poly-nitro component and the surrounding environment, if the surrounding molecule/ion forms a framework to trap these poly-nitro components, their thermostability is improved. For example, the thermostablity of DN was improved to 221 °C through encapsulation of energetic MOFs,[14] and the decomposition temperature of the nitroformate was improved to 200 °C through encapsulation of HOFs.[10] Although there is only one encapsulated example for both DN and NF (one for each), their thermostability is still undesirable. These two examples suggest strongly that encapsulation is a very promising strategy to improve the thermostablilty of the poly-nitro component to a higher level with a desirable stability.

Supramolecules, which can be constructed readily through non-covalent interactions between components, have played an extensive role in molecular cognition, delivery, stabilization, *etc.*[15–17] Moreover, supramolecules in which the components are

[a]Department of Chemistry, University of Idaho, Moscow, Idaho 83844-2343, USA
[b]Sauvage Laboratory for Smart Materials, Harbin Institute of Technology, Shenzhen 518055, China
[c]School of Petrochemical Engineering, Changzhou University, Changzhou 213000, China
[d]Department of Chemistry, Michigan State University, East Lansing, Michigan 48824, USA

† Electronic supplementary information (ESI) available: Preparation method, single crystal information, hydrogen bond information of anion, hydrogen bond frame structure of anion, DSC and TG curves, NCI and ESP calculations, Hirshfeld surfaces, computation and properties. CCDC 1992837, 1992828, 2298704–2298707. For ESI and crystallographic data in CIF or other electronic format see DOI: https://doi.org/10.1039/d3ta07665b

paired through a hydrogen bond synthon form a tight framework with excellent stability.[18–20] Hence, if the poly-nitro oxidant component is encapsulated by a supramolecular framework consisting of paired hydrogen bonds, and the poly-nitro components form hydrogen bonds with the surrounding supramolecular ligands, the decomposition temperature of the poly-nitro component will be remarkably improved. Fortunately, poly-amino heterocyclic rings meet the requirement from the energetic materials' point perfectly, since not only N and NH_2 from different poly-amino-heterocyclic ligands connect them into supramolecular frameworks through paired hydrogen bonds, and the NH_2 group in a ligand can also form various hydrogen bonds with the encapsulated poly-nitro components.[21,22]

Now, considering the cost and solubility, melamine was selected for assembly with DN, and the supramolecular structure with the encapsulated dinitramide MA@DN was obtained in aqueous solution. The poly-nitro components were then extended to NF and TNP, which have more nitro groups (Scheme 1). It is exciting that the supramolecular structures MA@NF, and MA@TNP with encapsulated NF and TNP were obtained, respectively. Enlightened by the above statement and discovery, TATOT with a high heat of formation was selected to assemble with the three poly-nitro components, respectively, in order to improve the energy density of the resultant supramolecules. Subsequently, all three poly-nitro components were successfully encapsulated forming supramolecular structures TATOT@DN, TATOT@NF and TATOT@TNP. The decomposition temperatures of MA@DN, MA@NF, MA@TNP, TATOT@DN, TATOT@NF, and TATOT@TNP are 243 and 225, 268, 225, 182 and 222 °C, respectively. The thermostabilities of MA@DN, MA@NF, and TATOT@TNP are the highest among those derivatives of DN, NF, and TNP, respectively. Their structures, and detonation properties as well as physicochemical properties, were studied comprehensively in this work.

Results and discussion

Single crystal structures

MA@DN crystalizes in a triclinic ($P\bar{1}$) space group with two molecules of H_2O, one dinitramide anion, two melamine cations (50% occupancy of proton in melamine), to give a formula $\{(C_3H_{6.5}N_{6.})_2 \cdot N(NO_2)_2 \cdot 2H_2O\}_n$, with a density of 1.668 g cm^{-3} at 173 K {ESI (ESI), Section S2†}. Each dinitramide anion was encapsulated by six half-melamine cations located on both sides of the DN (Fig. 1a and b); the four O atoms of each DN were fixed by 6H bonds from the surrounding six melamine cations, with lengths ranging from 2.132 Å to 2.501 Å (ESI, Sections S3 and S4†). The half-melamine cations were connected by paired H bonds with lengths of 2.105 and 2.129 Å, respectively, to form the supramolecular framework. Finally, the supramolecular framework and its encapsulated DN form a 2D planar network *via* various hydrogen bonds (Fig. 1c).

MA@NF and MA@TNP were prepared in the same way as MA@DN, which is shown in Fig. 2. MA@NF also crystallized in a triclinic ($P\bar{1}$) space group, with one H_2O, one nitroform anion, one melamine cation, and one neutral melamine in each unit cell (Formula: $C_3H_6N_6 \cdot C_3H_7N_6 \cdot C(NO_2)_3 \cdot H_2O$) with a density of 1.715 g cm^{-3} at 173 K. Similar to the structure of MA@DN, the melamine molecule and its cations were connected into supramolecular framework through parallel H bonds (from 2.120 Å to 2.215 Å), the supramolecular frameworks which were arranged on both sides of the NF anion, and all oxygen atoms of the NF anion were trapped by the supramolecular framework through nine (9) H bonds (from 2.154 Å to 2.536 Å, Fig. 2a and b). The larger volume of NF compared to that of DN, leads to one oxygen of a nitro group extending out of the supramolecular plane. Finally, the NF anions, the melamine molecules and the melamine cations were connected by these H bonds into a 2D supramolecular network (Fig. 2c). MA@TNP also crystallized in a triclinic ($P\bar{1}$) space group, with two H_2O molecules, one nitroform anion, one melamine cation, and one neutral melamine in each unit cell (Formula: $C_3H_6N_6 \cdot C_3H_7N_6 \cdot C_3N_5O_6 \cdot 2H_2O$) with a density of 1.655 g cm^{-3} at 100 K. Similarly, melamine and its cations were connected by parallel H bonds (from 1.959 Å to 2.214 Å) into a supramolecular framework arranging both sides of the TNP anion. The TNP anion was trapped by the supramolecular framework which formed though 6H bonds (5H bonds on one side and 1H bond on the other side (Fig. 2d and e)), whose lengths are between 1.968 Å and 2.472 Å. Similar to MA@NF, the steric hindrance of the three adjacent nitro groups of TNP causes one nitro group to extend out of the supramolecular plane. Nevertheless, TNP anions and the supramolecular framework which formed were in a 2-D network (Fig. 2f).

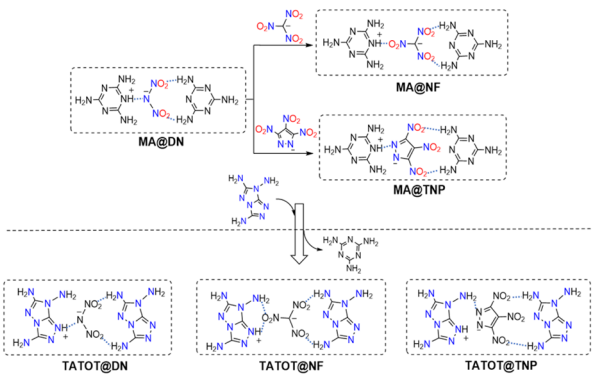

Scheme 1 Assembly of supramolecular structures with encapsulated poly-nitro oxidant components.

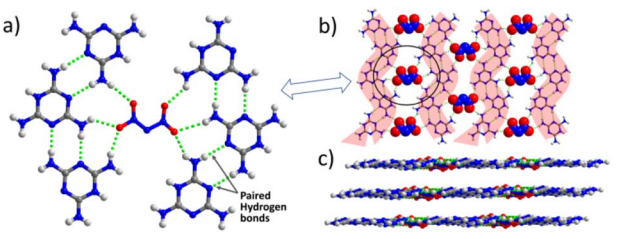

Fig. 1 (a) The surrouding hydrogen bonding enviroment of NF in MA@DN; (b) the supramolecular encapsulated structure of MA@DN; (c) the layer by layer packing of MA@DN.

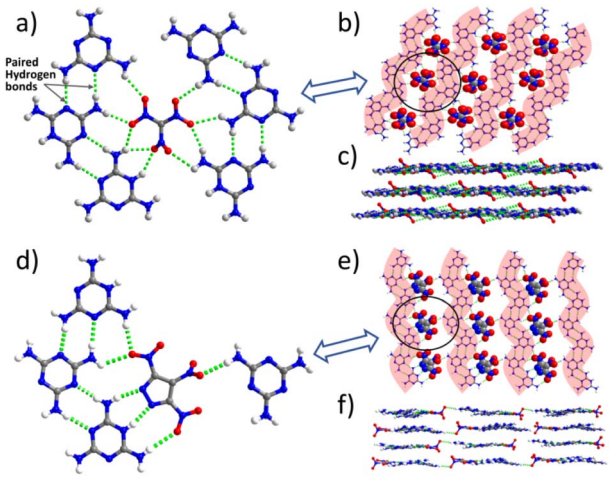

Fig. 2 Single crystal structures and packing modes of supramolecular structures MA@NF (2a)–(2c) and MA@TNP (2d)–(2f) (H_2O molecules are omitted).

Screened by the poly-amino heterocyclic ring, acceptable solubility, high heat of formation, and simple preparation, 3,6,7-triamino-7*H*-[1,2,4]triazolo[5,1-*c*][1,2,4]-triazole (TATOT, 470.5 kJ mol^{-1})[13] was selected to replace MA to assemble with DN, NF and TNP anions, respectively. Interestingly, TATOT assembled encapsulated supramolecular structures TATOT@DN ($C_3H_6N_8 \cdot C_3H_7N_8 \cdot N(NO_2)_2$), TATOT@NF ($C_3H_6N_8 \cdot C_3H_7N_8 \cdot C(NO_2)_3$), and TATOT@TNP ($(C_3H_{6.5}N_8)_2 \cdot C_3N_5O_6 \cdot 2H_2O$) with all these three anions. X-ray single-crystal diffraction shows that these three supramolecular structures crystallized in a triclinic ($P\bar{1}$) space group with calculated densities of 1.743, 1.722 and 1.741 g cm^{-3} at 100 K, respectively. Similar to the series of MA-based supramolecules, in all these three structures, TATOT and its cations formed linear supramolecular structures through paired H bonds, and the anions were encapsulated by linear supramolecular structures from both sides through H bonds (Fig. 3). Different from the single poly-nitro anion encapsulation in the MA series, each of two anions were trapped by supramolecular structures in the TATOT series. It is interesting that in TATOT@DN and TATOT@NF, all of the oxygen atoms of DN and NF were fixed by 10 and 8H bonds, respectively. It is possible that due to the bigger volume and more crowded nitro groups in TNP compared to that of DN and NF, three and one oxygen atom(s) of TNP are not fixed by H bonds in MA@TNP and TATOT@TNP, respectively. Finally, all these three encapsulated structures were connected to be 3-D supramolecules by H bonds (Fig. S1–S3†).

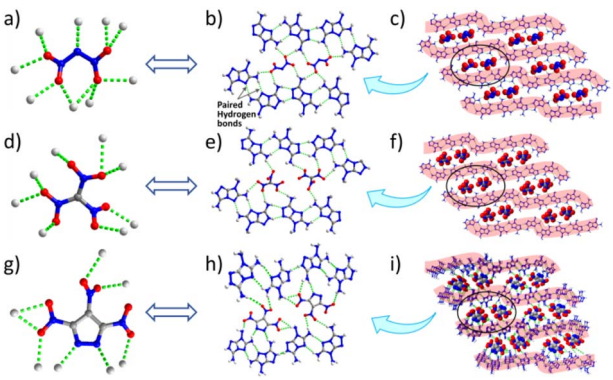

Fig. 3 Single crystal structures and packing modes of TATOT@DN (a)–(c), TATOT@NF (d)–(f), and TATOT@TNP (g)–(i) (H_2O molecules are omitted).

Stability

The poly-nitro components were encapsulated by supramolecular structures, and the poly-nitro component was fixed by H bonds. Their thermostabilities were determined under nitrogen at 5 °C min^{-1}. Although in the crystal structures of MA@DN, MA@NF, MA@TNP and TATOT@TNP, there is crystal H_2O, their thermal behaviors are almost the same as those of the anhydrous samples (supplementary section 5†), except for the disappearance of the endothermic H_2O peak which suggests that the removal of the lattice water molecule doesn't change the supramolecule structure. It is exciting that all six supramolecules have excellent thermostabilities, with decomposition temperatures (onset) at 243, 225, 268, 225, 182, and 222 °C (Fig. 4), respectively.

The thermostablities of MA@DN, MA@NF, and MA@TNP are the highest among their derivatives, respectively. The impact and friction sensitivities of these dried samples were determined by BAM standards, and for the supramolecules based on the MA series, all of them are insensitive to impact and friction (IS > 40 J, FS > 360 N). The impact sensitivities of TATOT@DN, TATOT@NF, and TATOT@TNP are 30 J, 25 J and 25 J, respectively, and all of them are insensitive to friction (FS > 360 N). Although the decomposition temperatures of the supramolecules based on TATOT are lower than those of the MA series, they are higher than the majority of DN, NF and TNP derivatives, respectively. High thermostabilities and less sensitivity to external stimulation suggest that all six supramolecules are full of potential.

Given the excellent stabilities of the supramolecules, it was interesting to investigate the rationale for their high thermal stabilities. Compared with the crystal structures of TABT-DN,[13] MA-NF[3] and TATOT-TNP,[23] which have high decomposition temperatures (201 °C, 143 °C and 208 °C, respectively) for the DN,[12] NF[2–9] and TNP[24] salts, respectively, the strength of the

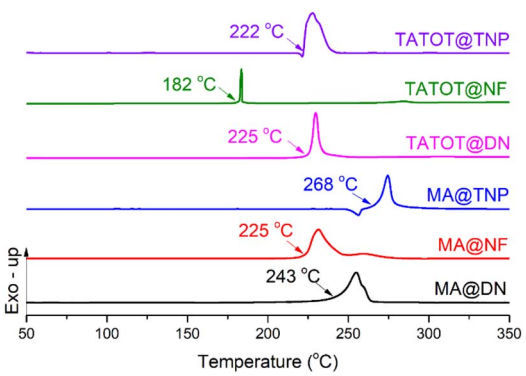

Fig. 4 The differential scanning calorimetry (DSC) scans of the six supramolecules at 5 °C min^{-1} in a N_2 atmosphere.

supramolecular structures which are connected by paired H bonds are stronger (Fig. 1–3), was proved by the NCI (Noncovalent interaction) calculations (Fig. 5a–h and ESI, Section S6†).[25,26] Additionally, NCI calculations also show that the encapsulated poly-nitro component has multi-interactions with the supramolecular framework. Particularly, in MA@DN, MA@NF, TATOT@DN and TATOT@NF, each oxygen atom of an NO_2 group has noncovalent interactions with the supramolecular frameworks. In these four supramolecules, the noncovalent interactions between the poly-nitro oxidants are stronger than other structures based on DN and NF, respectively. For the DN series of supramolecules, the interactions between DN and the supramolecular framework which consisted of MA are stronger than that in TATOT@DN. Similarly, the interactions between NF and the supramolecular framework consisting of MA is stronger than that in TATOT@NF. Calculations based on ESP (Electrostatic Potential) show that the maximum ESP around DN and NF in MA@DN and MA@NF are 41.14 and 43.39 kcal mol^{-1} (Fig. 5i–l), respectively, which are lower than those in TATOT@DN (41.78 kcal mol^{-1}) and TATOT@NF (49.87 kcal mol^{-1}), rationalizing that the decomposition temperatures of MA@DN and MA@NF are higher than those of TATOT@DN and TATOT@NF,[27,28] respectively. ESP calculations also support that the observed thermostable order for the DN and NF series are MA@DN > TATOT@DN > TABT-DN, MA@NF > MA-TATOT@NF[10] >TATOT@NF > MA-NF,[3] respectively. 2D fingerprint calculations based on Hirshfeld surfaces show that higher percentages of O···O interactions result in the lower stability, which is due to that the fact that more O···O interactions mean more NO_2 groups are not trapped and fixed by surrounding ligands.[29] For example, in the DN series, the O···O interactions of MA@DN > TATOT@DN > TABT-DN are 0.7, 0.9 and 2.3% (Fig. 6 and Supplementary section 7†), respectively, which explains the thermostable order of MA@DN > TATOT@DN > TABT-DN.

Detonation properties

The densities of the six anhydrous supramolecules were determined at room temperature to be 1.68, 1.72, 1.66, 1.69, 1.68 and 1.74 g cm^{-3}, respectively (Table 1). Their heats of formation were calculated to be 7.9, −390.7, −487.3, 1206.0, 868.5, and 782.4 kJ mol^{-1} (Supplementary section 8†), respectively, according to the method of literature.[30] Their detonation velocities were determined by EXPLO5 (6.06.02 version) to be 7663, 7345, 6540, 9388, 8838, and 8433 m s^{-1}, respectively, and the detonation pressures are 20.19, 18.55, 14.10, 36.52, 32.15, and 28.65 GPa, respectively. Except for MA@TNP, all the detonation properties of the new supramolecules are higher than those of TNT.[26] Supramolecules of the TATOT series have excellent detonation properties, *e.g.*, the detonation properties of TATOT@NF are comparable to

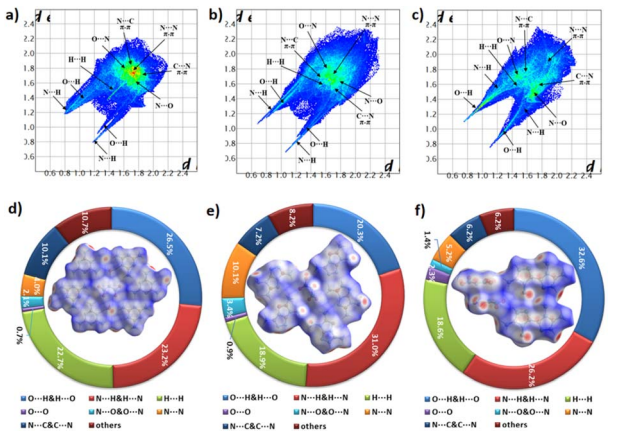

Fig. 6 2D fingerprint calculations and its statistics of interaction types for the DN series.

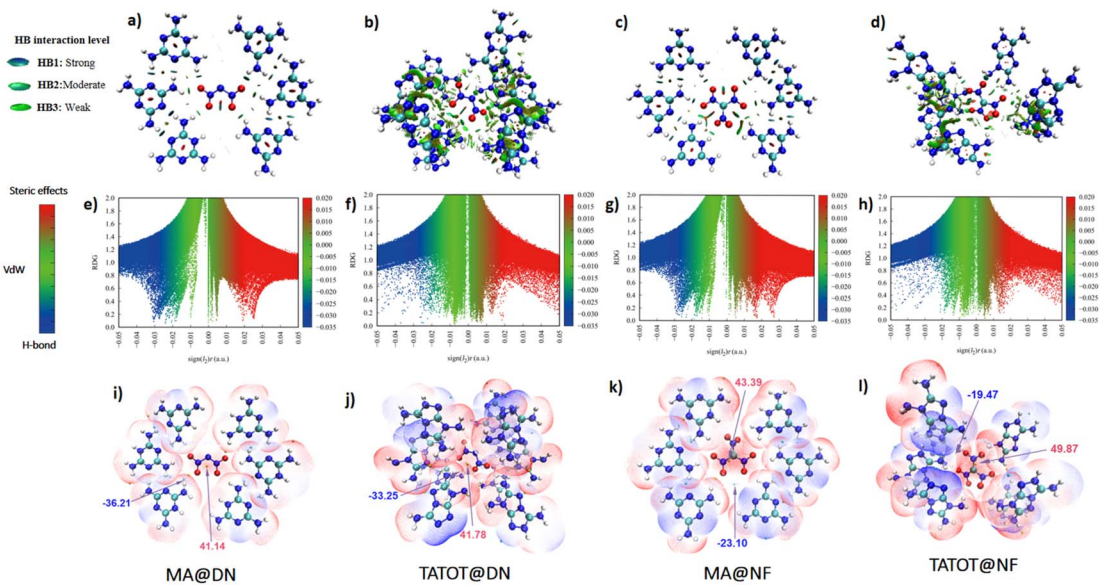

Fig. 5 (a–h) NCI calculations of MA@DN, TATOT@DN, MA@NF and TATOT@NF; (i–l) the ESP calculations of MA@DN, TATOT@DN, MA@NF and TATOT@NF.

Table 1 Physicochemical properties of different energetic compounds

Supramolecule	ρ^a (g cm^{-3})	$T_d{}^b$ (°C)	$\Delta H_f{}^{o\ c}$ (kJ mol^{-1})	$D_v{}^d$ (m s^{-1})	P^e (GPa)	IS^f (J)	FS^g (N)
MA@DN	1.68	243	7.9	7663	20.19	>40	>360
MA@NF	1.72	225	−390.7	7345	18.55	>40	>360
MA@TNP	1.66	268	−487.3	6540	14.18	>40	>360
TATOT@DN	1.69	225	1206.0	9388	36.52	30	>360
TATOT@NF	1.68	182	868.5	8838	32.51	25	>360
TATOT@TNP	1.74	222	782.4	8433	28.65	28	>360
TNT[h]	1.65	295	−115	6881	19.50	15	353
RDX[i]	1.81	205	80	8750	34.9	7.5	120
HMX[j]	1.91	270	74.8	9144	39.20	7.5	120

[a] Experimental density at room temperature. [b] Decomposition temperature (onset) (°C). [c] Enthalpy of formation (kJ mol^{-1}). [d] Detonation velocity (m s^{-1}). [e] Detonation pressure (GPa). [f] Impact sensitivity (J). [g] Friction sensitivity (N). [h] Ref. 15. [i] Ref. 19. [j] Ref. 20.

that of RDX,[31] and the detonation velocity of TATOT@DN is comparable to that of HMX.[32] All six supramolecular structures are promising candidates for energetic materials due to their excellent thermostabilities.

Conclusions

A new strategy for encapsulating poly-nitro components through supramolecular self-assembly was discovered. Six supramolecular structures of MA@DN, MA@NF, MA@TNP.

TATOT@DN, TATOT@NF, and TATOT@TNP were simply obtained in an aqueous solution. Benefiting from the supramolecular framework, and tight encapsulation by supramolecular structures though H bonds, the thermostability of these poly-nitro components was improved remarkably. In particular, the decomposition temperatures of MA@DN, MA@NF, and MA@TNP are 243, 225, and 268 °C, respectively, which are the highest among their corresponding derivatives. Additionally, the TATOT series of supramolecules have excellent detonation properties, which gives them a good potential to behave as energetic materials. Since this study provides a novel insight and strategy for stabilizing poly-nitro components, more and more poly-nitro oxidants with high thermostability and excellent properties will be designed and prepared based on this work.

Author contributions

Jichuan Zhang, Jiaheng Zhang and Jean'ne M. Shreeve designed the study. Jichuan Zhang performed most of the experiments and measurements. Jinhao Zhang and Jatinder Singh completed the theoretical calculations. Richard J. Staples performed crystallographic structural analysis. Wanbao Wu contributed to the discussion writing. Jichuan Zhang, Jiaheng Zhang, and Jean'ne M. Shreeve prepared the manuscript.

Conflicts of interest

There are no conflicts to declare.

Acknowledgements

The Rigaku Synergy S Diffractomer was purchased with support from the National Science Foundation MRI program (1919565). The authors are grateful to the Fluorine-19 Fund. This work was financially supported by the National Natural Science Foundation of China (Grant No. 21905069, 22208073, U21A20307), the Shenzhen Science and Technology Innovation Committee (Grant No. ZDSYS20190902093220279, KQTD20170809110344233, GXWD20201230155427003-20200821181245001, GXWD20201230155427003-20200821181809001, ZX20200151), the Department of Science and Technology of Guangdong Province (Grant No. 2020A1515110879).

References

1 K. O. Christe, W. W. Wilson, M. A. Petrie, H. H. Michels, J. C. Bottaro and R. Gilardi, *Inorg. Chem.*, 1996, **35**(17), 5068–5071.
2 Y. Huang, H. Gao, B. Twamley and J. M. Shreeve, *Eur. J. Inorg. Chem*, 2007, 2025–2030.
3 M. Göbel and T. M. Klapötke, *Z. Anorg. Allg. Chem.*, 2007, **633**(7), 1006–1017.
4 Q.-H. Lin, Y.-C. Li, Y.-Y. Li, Z. Wang, W. Liu, C. Qi and S.-P. Pang, *J. Mater. Chem.*, 2012, **22**(2), 666–674.
5 Q.-H. Lin, Y.-C. Li, C. Qi, W. Liu, Y. Wang and S.-P. Pang, *J. Mater. Chem. A*, 2013, **1**(23), 6776–6785.
6 W. Liu, S.-H. Li, Y.-C. Li, Y.-Z. Yang, Y. Yu and S.-P. Pang, *J. Mater. Chem. A*, 2014, **2**(38), 15978–15986.
7 J.-T. Wu, J.-G. Zhang, X. Yin, Z.-Y. Cheng and C.-X. Xu, *New J. Chem.*, 2015, **39**(7), 5265–5271.
8 A. F. Baxter, I. Martin, K. O. Christe and R. Haiges, *J. Am. Chem. Soc.*, 2018, **140**(44), 15089–15098.
9 Y. Du, H. Su, T. Fei, B. Hu, J. Zhang, S. Li, S. Pang and F. Nie, *Cryst. Growth Des.*, 2018, **18**(10), 5896–5903.
10 J. Zhang, Y. Feng, R. J. Staples, J. Zhang and J. M. Shreeve, *Nat. Commun.*, 2021, **12**(1), 2146.
11 B. Wang, Y. Feng, X. Qi, M. Deng, J. Tian and Q. Zhang, *Chem.–Eur. J.*, 2018, **24**(59), 15897–15902.
12 S. Venkatachalam, G. Santhosh and K. Ninan, *Propellants Explos. Pyrotech.*, 2004, **29**(3), 178–187.

13 T. M. Klapötke, P. C. Schmid, S. Schnell and J. Stierstorfer, *J. Mater. Chem. A*, 2015, **3**(6), 2658–2668.
14 J. Zhang, Y. Du, K. Dong, H. Su, S. Zhang, S. Li and S. Pang, *Chem. Mater.*, 2016, **28**(5), 1472–1480.
15 C. T. Seto and G. M. Whitesides, *J. Am. Chem. Soc.*, 1993, **115**(3), 905–916.
16 D. L. Caulder and K. N. Raymond, *Acc. Chem. Res.*, 1999, **32**(11), 975–982.
17 D. B. Amabilino, D. K. Smith and J. W. Steed, *Chem. Soc. Rev.*, 2017, **46**(9), 2404–2420.
18 G. R. Desiraju, *Angew. Chem., Int. Ed.*, 1995, **34**(21), 2311–2327.
19 L. S. Reddy, N. J. Babu and A. Nangia, *Chem. Commun.*, 2006, **13**, 1369–1371.
20 N. R. Goud, N. J. Babu and A. Nangia, *Cryst. Growth Des.*, 2011, **11**(5), 1930–1939.
21 P. Li, O. Alduhaish, H. D. Arman, H. Wang, K. Alfooty and B. Chen, *Cryst. Growth Des.*, 2014, **14**(7), 3634–3638.
22 P. Li, H. D. Arman, H. Wang, L. Weng, K. Alfooty, R. F. Angawi and B. Chen, *Cryst. Growth Des.*, 2015, **15**(4), 1871–1875.
23 P. Yin, J. Zhang, D. A. Parrish and J. M. Shreeve, *J. Mater. Chem. A*, 2015, **3**(16), 8606–8612.
24 Y. Zhang, Y. Guo, Y. H. Joo, D. A. Parrish and J. M. Shreeve, *Chem.–Eur. J.*, 2010, **16**(35), 10778–10784.
25 E. R. Johnson, S. Keinan, P. Mori-Sánchez, J. Contreras-García, A. J. Cohen and W. Yang, *J. Am. Chem. Soc.*, 2010, **132**(18), 6498–6506.
26 J. Zhang, Q. Zhang, T. T. Vo, D. A. Parrish and J. M. Shreeve, *J. Am. Chem. Soc.*, 2015, **137**(4), 1697–1704.
27 S. Grimme, S. Ehrlich and L. Goerigk, *J. Comput. Chem.*, 2011, **32**(7), 1456–1465.
28 Y. Wang, Y. Liu, S. Song, Z. Yang, X. Qi, K. Wang, Y. Liu, Q. Zhang and Y. Tian, *Nat. Commun.*, 2018, **9**(1), 2444.
29 M. A. Spackman and D. Jayatilaka, *CrystEngComm*, 2009, **11**(1), 19–32.
30 Y. Wang, S. Song, C. Huang, X. Qi, K. Wang, Y. Liu and Q. Zhang, *J. Mater. Chem. A*, 2019, **7**(33), 19248–19257.
31 J. Zhang, Y. Feng, Y. Bo, A. K. Chinnam, J. Singh, R. J. Staples, X. He, K. Wang, J. Zhang and J. M. Shreeve, *Chem*, 2022, **8**(10), 2678–2687.
32 J. Zhang, Y. Feng, Y. Bo, R. J. Staples, J. Zhang and J. M. Shreeve, *J. Am. Chem. Soc.*, 2021, **143**(32), 12665–12674.